ISSN 1674-1056
http://cpb.iphy.ac.cn
http://iopscience.iop.org/cpb
中国物理 B
Chinese Physics
中国物理
Chinese Physics B

Reduced graphene oxide as saturable absorbers for erbium-doped passively mode-locked fiber laser

Zhen-Dong Chen(陈振东), Yong-Gang Wang(王勇刚), Lu Li(李 璐), Rui-Dong Lv(吕瑞东), Liang-Lei Wei(韦良雷), Si-Cong Liu(刘思聪), Jiang Wang(王 江), Xi Wang(王茜)

Citation: Chin. Phys. B . 2018, 27(8): 084206. **doi:** 10.1088/1674-1056/27/8/084206

Journal homepage: http://cpb.iphy.ac.cn; http://iopscience.iop.org/cpb

What follows is a list of articles you may be interested in

Generation of single and multiple dissipative soliton in an erbium-doped fiber laser

Li-Na Duan(段利娜), Jin Wen(文进), Wei Fan(樊伟), Wei Wang(王炜)

Chin. Phys. B . 2017, 26(10): 104205. **doi:** 10.1088/1674-1056/26/10/104205

Fiber fuse behavior in kW-level continuous-wave double-clad field laser

Jun-Yi Sun(孙骏逸), Qi-Rong Xiao(肖起榕), Dan Li(李 丹), Xue-Jiao Wang(王雪娇), Hai-Tao Zhang(张海涛), Ma-Li Gong(巩马理), Ping Yan(闫平)

Chin. Phys. B . 2016, 25(1): 014204. **doi:** 10.1088/1674-1056/25/1/014204

Yb-doped passively mode-locked fiber laser with Bi_2Te_3-deposited

Li Lu, Yan Pei-Guang, Wang Yong-Gang, Duan Li-Na, Sun Hang, Si Jin-Hai

Chin. Phys. B . 2015, 24(12): 124204. **doi:** 10.1088/1674-1056/24/12/124204

Passive harmonic mode-locking of Er-doped fiber laser using CVD-grown few-layer MoS_2 as a saturable absorber

Xia Han-Ding, Li He-Ping, Lan Chang-Yong, Li Chun, Deng Guang-Lei, Li Jian-Feng, Liu Yong

Chin. Phys. B . 2015, 24(8): 084206. **doi:** 10.1088/1674-1056/24/8/084206

Influences of cavity dispersion distribution on the output pulse properties of an all-normal-dispersion fiber laser

Li Pan, Shi Lei, Sun Qing, Feng Su-Juan, Mao Qing-He

Chin. Phys. B . 2015, 24(7): 074207. **doi:** 10.1088/1674-1056/24/7/074207

SPECIAL TOPIC — Nanophotonics

Reduced graphene oxide as saturable absorbers for erbium-doped passively mode-locked fiber laser*

Zhen-Dong Chen(陈振东)[1], Yong-Gang Wang(王勇刚)[1,†], Lu Li(李璐)[2], Rui-Dong Lv(吕瑞东)[1], Liang-Lei Wei(韦良雷)[1], Si-Cong Liu(刘思聪)[1], Jiang Wang(王江)[1], and Xi Wang(王茜)[3]

[1] *School of Physics and Information Technology, Shaanxi Normal University, Xi'an* 710119, *China*
[2] *School of Science, Xi'an Institute of Posts and Telecommunications, Xi'an* 710121, *China*
[3] *State Key Laboratory of Transient Optics and Photonics, Xi'an Institute of Optics and Precision Mechanics, Chinese Academy of Sciences, Xi'an* 710119, *China*

(Received 2 February 2018; revised manuscript received 31 March 2018; published online 10 July 2018)

We demonstrate a nanosecond mode-locked erbium-doped fiber laser (EDFL) based on a reduced graphene oxide (RGO) saturable absorber (SA). The RGO SA is prepared by depositing the graphene oxide (GO) on fluorine mica through thermal reduction of GO. A scanning electron microscope (SEM), Raman spectrometer, and x-ray photoelectron spectroscopy (XPS) are adopted to analyze the RGO characteristics. The results show that the reduction degree of graphene oxide is very high. By embedding the RGO SA into the EDFL cavity, a stable mode-locked fiber laser is achieved with a central wavelength of 1567.29 nm and repetition rate of 12.66 MHz. The maximum output power and the minimum pulse duration are measured to be 18.22 mW and 1.38 ns respectively. As far as we know, the maximum output power of 18.22 mW is higher than those of other nanosecond mode-locked oscillators reported. Such a nanosecond pulse duration and megahertz repetition rate make this mode-locked erbium-doped fiber laser a suitable seed oscillator for high-power applications and chirped pulse amplifications.

Keywords: fiber lasers, mode-locked pulse, nonlinear optical materials, reduced graphene oxide

PACS: 42.55.Wd, 42.60.Fc, 42.70.Nq **DOI:** 10.1088/1674-1056/27/8/084206

1. Introduction

Passive mode-locked fiber lasers in the near-infrared region possess many practical applications in optical communication, medicine, metrology, and material processing because of their simple compact design and good beam.[1–4] The passive mode-locking is usually established through the saturable absorbers, such as semiconductor saturable absorber mirrors (SESAMs),[5,6] nonlinear optical loop mirror, nonlinear polarization rotation technique (NPR),[7] carbon nanotube,[8,9] graphene,[10–14] etc.[15–19] Recently, some new two-dimensional (2D) materials were confirmed as saturable absorbers for mode-locking operation in the laser, such as black phosphorus[20–22] MXene,[23] antimonene,[24] etc. Because every material has its own advantages, it is attractive to explore more mode-locked absorber materials, such as MXene, which has a wide saturated absorptive range, including the near-far infrared region due to metallic characteristics. The stability of antimonene is good and the nonlinear refractive index is relatively large. Although graphene has been widely studied in laser applications, the thermal reduction graphene oxide is less used in lasers. The preparation technology of graphene is more mature than those of other new 2D materials. Especially the zero-bandgap of graphene makes it a broadband saturable absorber for any wavelength of light.[25] Therefore, it is necessary to further study the application of graphene in the laser.

Graphene saturable absorbers can be prepared by many methods, such as chemical vapor deposition (CVD), peeling graphite, and reduction-oxidation methods.[26,27] The CVD-graphene can be grown on substrates, and then easily transferred to a fiber connector. The graphene can also be directly grown on D-type fiber or taper fiber by CVD.[28] However, the yield of the graphene prepared in this method is low and the preparation process is very complex. Peeling graphite is the simplest way to prepare graphene, such as liquid phase exfoliation, the mechanical exfoliation method, etc. However, the repeatability of the process is very poor. The reduction–oxidation method is the most widely used method of preparing the graphene: graphite oxide is obtained by oxidizing and exfoliating graphite, then graphene can be obtained by reduction reaction of graphite oxide. The problem is that the degree of reduction prepared in this way is generally not high.[29] In this work, we use the method of thermal reduction reaction to prepare RGO with high reduction degree.

Up to now, investigation of mode-locked EDFL have mainly been focused on emitting picosecond or femtosecond

*Project supported by the Central University Special Fund for Basic Research and Operating Expenses, China (Grant No. GK201702005), the Natural Science Foundation of Shaanxi Province, China (Grant No. 2017JM6091), the National Natural Science Foundation of China (Grant No. 61705183), and the Fundamental Research Funds for the Central Universities (Grant No. 2017TS011).

†Corresponding author. E-mail: chinawygxjw@snnu.edu.cn

© 2018 Chinese Physical Society and IOP Publishing Ltd

pulses.[30–33] However, nanosecond pulsed EDFL has advantages of large pulse width, low peak power, and little nonlinear phase accumulation. So it is more suitable for chirped pulse amplification systems than an ultrashort pulse fiber laser, though the passive mode-locked fiber laser with a low repetition rate has attracted a lot of attention for producing nanosecond pulses recently.[34–36] Li *et al.* generated the nanosecond dual-pulse with a repetition rate of 783.3 kHz based on the NPR technique.[34] Xu *et al.* demonstrates that mode-locked nanosecond EDFL with a graphen saturable absorber can produce a laser with a duration ranging from 3 ns to 20 ns by increasing the laser cavity length from 133 m to 1027 m.[35] Moreover, Wu *et al.* reported an 18.5-ns pulse at a 126-kHz repetition rate generated from a mode-locked erbium-doped fiber laser with the NPR technique in a ring cavity.[36] However, fiber laser with a long cavity cannot fully meet the needs of various applications, for example, laser with a low repetition rate generally has high single pulse energy, which leads to being damage in operation. A nanosecond mode locked fiber laser with high frequency has not been fully excavated.

In this work, we demonstrate that graphene oxide could be completely reduced at 1000 °C for 5 min. In this way we fabricate the reduced graphene oxide saturable (RGO) absorber based on fluorine mica (FM) substrate. By employing the RGO/FM absorber, a stable mode-locked fiber laser is achieved, with a resulting central wavelength of 1067.29 nm, repetition rate of 12.66 MHz, and pulse duration of 1.38 ns. The maximum output power is measured to be 18.22 mW. Considering the outstanding advantages of RGO, such as low cost, simple fabrication, and wavelength independence, the nanosecond erbium-doped fiber lasers based on RGO have a good prospect in practice.

2. RGO preparation and characterization

In this experiment, the GO aqueous solution was fabricated by the liquid phase exfoliation method as the following process. Firstly, 10-mg GO powder was poured into the deionized water and agitated for 8 h at an ultrasonic power of 360 W. The graphene oxide nanosheets were evenly dispersed into the water. Secondly, in order to isolate large particles, the mixed solution was centrifuged at 7000 rpm. The GO aqueous solution obtained is shown in Fig. 1(a). Finally, the graphene oxide solution was dropped on mica sheet (FM) and poured into a dry box for 1 h, then the GO/FM absorber was obtained. Through the exploration under different conditions, it is found that the graphene oxide could be completely reduced at 1000 °C for five min in a vacuum. The RGO/FM absorber prepared under such conditions is shown in Fig. 1(b).

The morphological characteristics of GO and RGO were characterized by SEM (Nova NanoSEM Training-X50 series). Figure 2(a) shows SEM images of GO, because the high flexibility of the GO layer causes the layer to deform, it can be observed that the surface of the graphene oxide is partially folded and undulated. The oxygen-containing functional groups attached to the chip layer make the dispersion of the lamellar layer better. Correspondingly, owing to the fact that the oxygen-containing functional groups on the surface are eliminated by reduction, the RGO layers present more serious folding and curling as shown in Fig. 2(b).

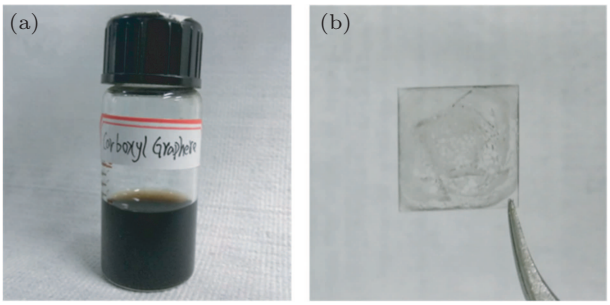


Fig. 1. (color online) (a) Suspension of the GO and (b) RGO/FM absorber.

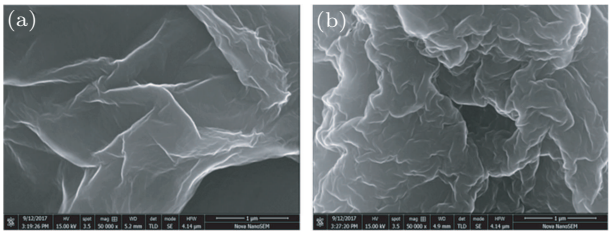


Fig. 2. SEM images of (a) GO and (b) RGO.

Raman spectroscopy is an effective tool for characterizing structural characteristics and properties of carbon nanomaterials. The microstructure of GO and RGO are investigated by Raman spectroscopy (LabRam confocal microprobe Raman system) as shown in Fig. 3, the test light source is the argon ion laser with a center wavelength of 532 nm. The peak of 1328 cm^{-1} is called the D peak, which is due to the defects in the carbon plane, reflecting the disorder structure of GO. The G peak at 1580 cm^{-1} is generated by the stretching vibration of the C–C bond, which is sensitive to the pressure of the system. The degree of graphitization of carbon nanomaterial is usually evaluated by the intensity ratio of D peak to G peak. The D/G intensity ratio of GO is 1.04, which shows that GO contains a lot of functional groups and the carbon layers are arranged orderly. When the GO is thermally reduced, the intensity of D peak increases, while the intensity of G peak begins to decrease. The D/G intensity ratio of RGO reaches to 1.32, which suggests that the thermal reduction of graphene oxide is successful.

The x-ray photoelectron spectroscopy (XPS) can be employed to determine the chemical environment of atoms. In order to further study the reduction degree of GO, XPS (AXIS ULTRA) is used to determine the content of different oxygen-containing functional groups in the GO structure. The C 1s XPS spectra of samples are fitted according to the peak position as shown in Fig. 4. It could be concluded that there are a hydroxyl

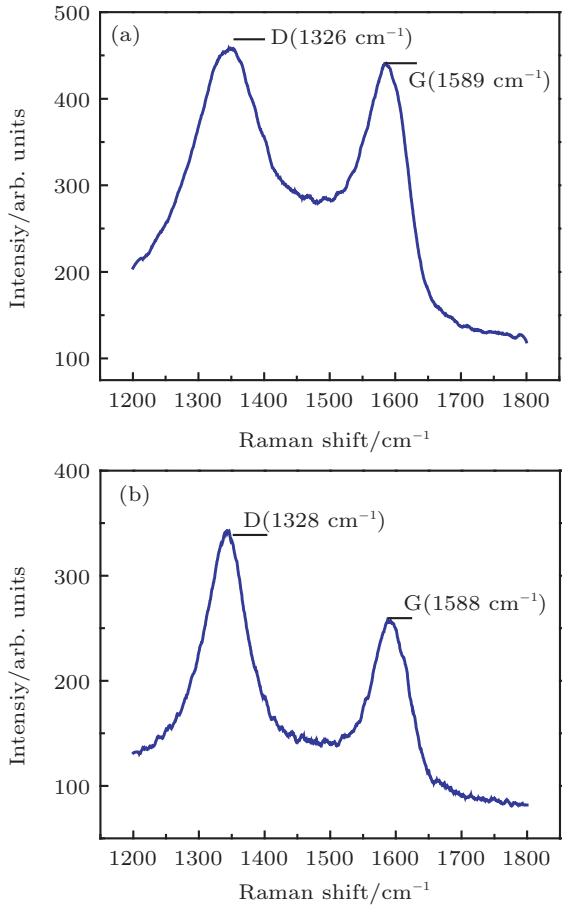


Fig. 3. (color online) Raman spectrum of (a) GO and (b) RGO.

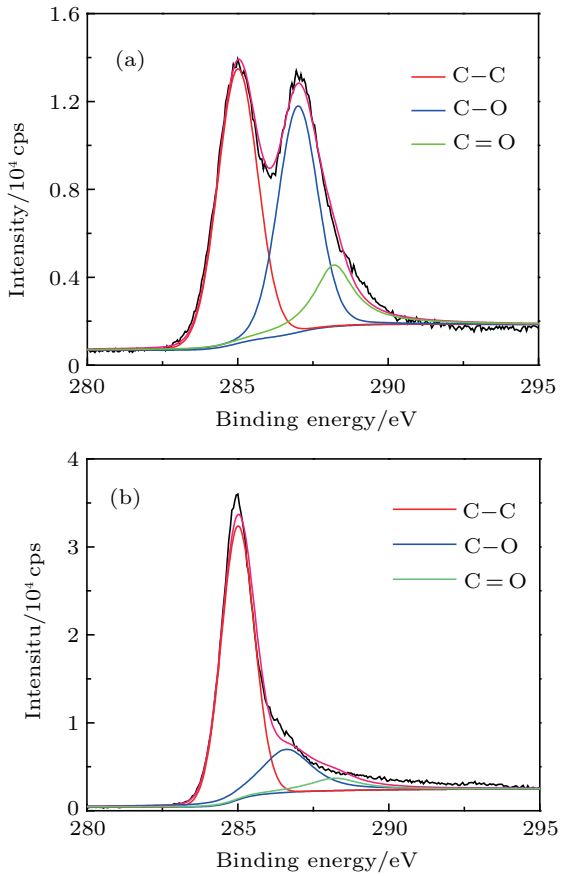


Fig. 4. (color online) C 1s XPS spectra of (a) GO and (b) RGO.

group and a carbonyl group in GO and the oxidation degree of graphene oxide is very high, so the GO can be easily stripped by the liquid phase exfoliation method. After high-temperature reduction of GO, the signal intensity of the C–C functional group with SP^2 hybrids of RGO increases, which explains that the percentage of area occupied by graphene is correspondingly raised. Meanwhile, carbonyl and hydroxyl groups decrease a lot. Furthermore, quantitative analysis of the XPS peak is provided in Tables 1 and 2. The content of the hydroxyl group is reduced from 39.59% to 22.39%, and correspondingly the content of the carbonyl group varies from 14.37% to 7.36%. It indicates that the structure of the carbon plane tends to be completely planar, and the functional groups are gradually removed. Figure 5 shows the corresponding peak intensities of the carbon and oxygen elements in the two groups of samples. The CC/CO intensity ratio of RGO (2.52) is higher than the CC/CO ratio of GO (0.79). The results also prove that the graphene oxide is fully reduced and also confirm the results obtained by the SEM and the Raman spectroscopy.

Table 1. XPS data of GO. BE is short for binding energy.

GO	Peak BE/eV	at.%	Bond
C 1s	285.0	45.64	C–C
C 1s	287	39.59	C–O (hydroxyl groups)
C 1s	288.2	14.37	C=O (carbonyl groups)

Table 2. XPS data of RGO.

RGO	Peak BE/eV	at.%	Bond
C 1s	285.0	70.25	C–C
C 1s	286.6	22.39	C–O (hydroxyl groups)
C 1s	288.2	7.36	C=O (carbonyl groups)

The linear transmission spectra of the RGO/FM absorber are measured from 1480 nm to 1580 nm. Figure 6(a) shows that the spectral transmission is always flat at a level of ∼76.5%±0.6%, and the linear optical absorption of the RGO/FM absorber is 76.1% at 1567.29 nm. In order to characterize the nonlinear saturable absorber property of RGO/FM SA, a home-made femtosecond pulsed EDF laser (working wavelength: 1560 nm; pulse width: 500 fs; pulse frequency: 26.23 MHz) was used as an illumination source. The modulation depth (ΔT) was measured to be 5.5% as shown in Fig. 6(b), which is suited to produce a mode-locked pulse.[37] It can also be obtained from Fig. 6(b) that the saturation power and non-saturable loss are 42 mW and 18.4%, respectively. The damage threshold of reduced graphene oxide based SA is measured by the femtosecond light source with a pulse width of 150 fs and pulse frequency of 10 kHz, which is 4.69 mJ/cm^2.

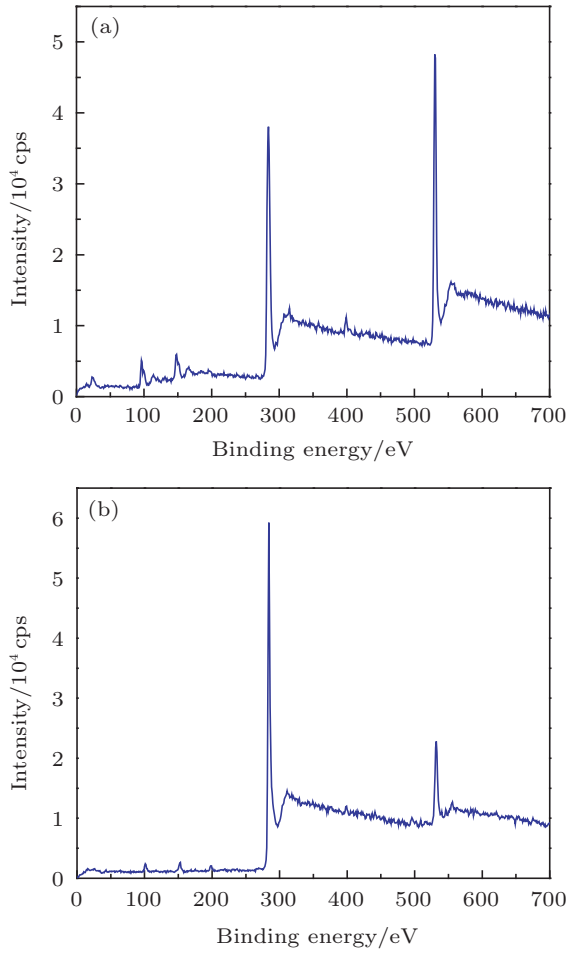


Fig. 5. (color online) XPS spectra of (a) GO and (b) RGO.

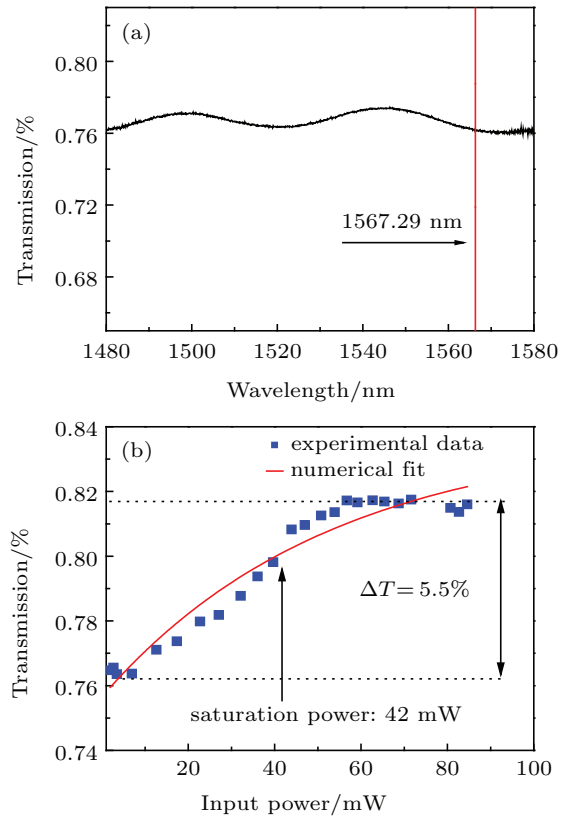


Fig. 6. (color online) (a) Linear transmission spectrum and (b) power-dependent transmission.

3. Laser setup and results

The experimental configuration of mode-locked erbium-doped fiber laser is schematically shown in Fig. 7. The ring laser oscillator cavity consists of a 750-mW/976-nm laser diode, a wave-length division multiplexer (WDM), a 3-m erbium-doped fiber, a polarization independent isolator (PI-ISO), an optical coupler (OC), a polarization controller (PC), and an RGO/FM absorber. A 3-m EDF with an absorption parameter of 25 dB/m at 1530 nm is employed as a gain medium and pumped by a 976-nm laser diode (LD). The PI-ISO is spliced in the cavity to guarantee the unidirectional operation and the eliminating of laser backscattering in the fiber ring cavity. A polarization controller (PC) is used to select different optical modes by inducing a birefringence in the fiber core, and 10% portion of the laser is coupled out from the laser cavity by the optical coupler. The pigtails of all the components are single mode fiber (SMF) with a total length of 13.14 m, the total ring cavity length is approximately 16.14 m. The output pulse train is observed by a power meter (JDSUOLP-85), an optical spectrum analyzer (Yokogawa AQ6370D), a 1-GHz digital oscilloscope (Rohde & Schwarz, RTO1014) with a home-made 5-GHz photodiode detector, and a 40-GHz radio-frequency analyzer (Agilent E4447A).

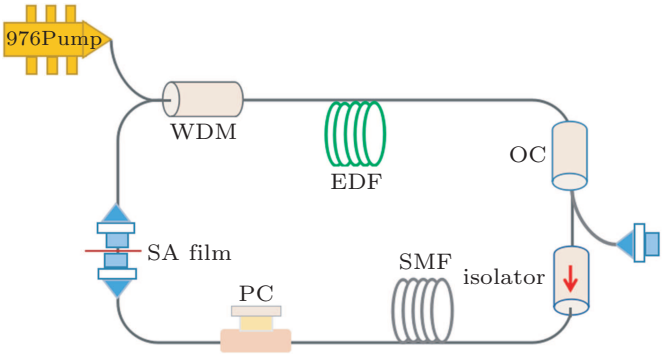


Fig. 7. (color online) Experimental setup of mode-locked laser.

In this experiment, continuous-wave (CW) operation is established at a pump power of 30 mW. Large inserting loss of the assembled RGO SA leads to high threshold of CW operation. After the appropriate adjustment of polarization controller, the laser starts to operate in the mode-locked regime with a pump power of 273 mW. When the pump power is increased to 635 mW, the mode-locked operation becomes unstable. However, the stable mode-locking operation is observed again by reducing the pump power to 550 mW. As shown in Fig. 8, the output power of the laser varies with pump power, and the output power increases linearly with pump power. When the pump power reaches to 635 mW, the maximum output power is obtained to be 18.22 mW, which corresponds to a single pulse energy of 1.44 nJ. In Table 3, we summarize the results of the nanosecond mode-locked fiber lasers in the last few years. As far as we know, the maximum

output power of 18.22 mW is higher than those obtained in other nanosecond mode-locked oscillators.[35,38–41]

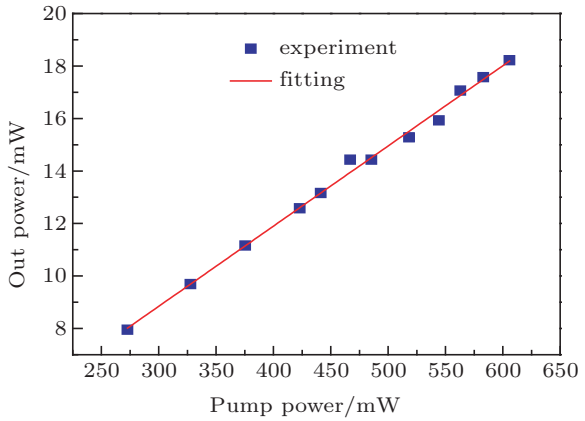


Fig. 8. (color online) Relationship between pump power and output power.

The output characteristics of the mode-locked laser are shown in Fig. 9 with a pump power of 563.07 mW. The recorded optical spectrum of the laser is shown in Fig. 9(a). The optical spectrum of fundamental mode-locked pulses is centered at 1567.29 nm and the 3-dB spectral width is 0.75 nm. The corresponding oscilloscope trace of the mode-locked pulse train is shown in Fig. 9(b), the time interval between the adjacent pulses is 78.99 ns, which agrees exactly with the cavity length of 16.14 m. During the experiments, we find that the pulse repetition rate 12.66 MHz remains unchangeable. When the pump power varies from 272.72 mW to 658.58 mW, the mode-locking state is not destroyed no matter how the pump power increases or decreases, which implies that the laser operates in the fundamental mode locking state rather than in the Q-switched state.[42,43] The pulse duration is measured to be 1.38 ns at a pump power of 563.07 mW as shown in Fig. 9(c). The RF spectrum of the mode-locked pulse reveals that the fundamental repetition frequency is located at 12.66 MHz as shown in Fig. 9(d). The signal-to-noise ratio (SNR) is 50 dB, which indicates that the mode-locked stability is good. The time-bandwidth product (TBP) is estimated at 126.405, which has a huge deviation with a transmission limit of 0.315. So we can confirm that the mode-locked pulses are heavily chirped.

Table 3. Typical nanosecond mode-locked fiber lasers.

SA	Repetition rate	Pulse duration	Maximum pulse energy	Output power	Ref.
Graphene	20 kHz-1540 kHz	3 ns–20 ns	1 nJ	0.38 mW	[35]
NPR	173.05 kHz	10 ns–1716 ns	41.8 nJ.	7.2 mW	[38]
Carbon-nanotube	909.1 kHz	332 ns	0.34 nJ	0.31 mW	[39]
Graphene oxide	7.68 MHz	4.85 ns	0.56 nJ	4.3 mW	[40]
Graphene	5.78 MHz	24 ns	2.1 nJ	12.1 mW	[41]
RGO	12.66 MHz	1.38 ns	1.44 nJ	18.22 mW	our work

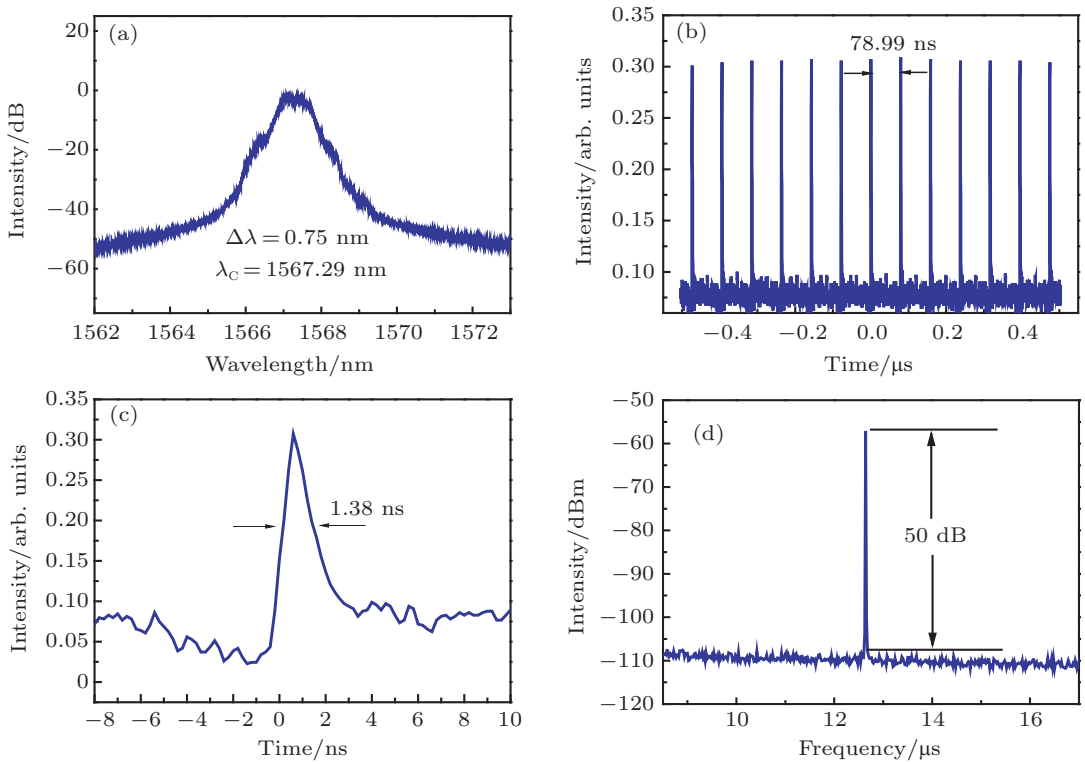


Fig. 9. (color online) Mode-locked pulse state, showing (a) optical spectrum, (b) pulse trains of oscilloscope, (c) single pulse of oscilloscope, and (d) radio-frequency spectrum.

Finally, in order to verify that the nanosecond mode-locked pulse is produced by the RGO SA instead of the self-locking effect, the RGO/FM is removed from the cavity. At the moment, the mode-locked pulse is not observed under the same experimental conditions, which indicates that the formation of nanosecond mode-locked pulse is generated by the nonlinear saturable absorber property of RGO in the cavity.

4. Conclusions and perspectives

In this research, we have prepared the RGO by the thermal reduction method. The RGO is characterized by SEM, Raman spectrometer, and XPS, and the results from determination and characterization indicate that the reduction degree of GO is very high. So we fabricate the RGO/FM absorber, and the modulation depth is measured to be 5.5%. By employing the RGO/FM absorber, a stable mode-locked fiber laser is achieved with a central wavelength of 1567.29 nm, repetition rate of 12.66 MHz, and pulse duration of 1.38 ns. The maximum output power is measured to be 18.22 mW. Hopefully, this kind of nanosecond fiber laser source with megahertz repetition rate will have a lot of potential applications.

References

[1] Keller U 2003 *Nature* **424** 831
[2] Sibbett W, Lagatsky A A and Brown C T A 2012 *Opt. Express* **20** 6989
[3] Brida D, Krauss G, Sell A and Leitenstorfer A 2014 *Laser Photon. Rev.* **8** 409
[4] Haus H A and Wong W S 1996 *Rev. Mod. Phys.* **68** 423
[5] Saraceno C J, Schriber C, Mangold M, Hoffmann M, Heckl O H, Baer C R E, Golling M, Sudmeyer T and Keller U 2012 *IEEE J. Sel. Top. Quantum Electron.* **18** 29
[6] Steinmeyer G, Sutter D H, Gallmann L, Matuschek N and Keller U 1999 *Science* **286** 1507
[7] Luo Z C, Xu W C, Song C X, Luo A P and Chen W C 2009 *Chin. Phys. B* **18** 2328
[8] Li X, Wang Y, Y, Zhao W, Yu X, Sun Z, Cheng X, Yu X, Zhang Y and Wang Q J 2014 *Opt. Express* **22** 17227
[9] Hasan T, Sun Z P, Wang F Q, Bonaccorso F, Tan P H, Rozhin A G and Ferrar A C 2009 *Adv. Mater.* **21** 3874
[10] Zhao X, Yan X Q, Ma Q, Zhang X L, Liu Z B and Tian J G 2013 *Acta Opt. Sin.* **33** 0719001 (in Chinese)
[11] Song Y F, Li L, Zhang H, Shen D Y and Loh K P 2013 *Opt. Express* **21** 10010
[12] Li H P, Zeng D B, Xia H D, Zhang S J, Tang X G and Liu Y 2013 *Laser Phys.* **23** 035102
[13] Popa D, Sun Z, Torrisi F, Hasan T, Wang F and Ferrari A C 2010 *Appl. Phys. Lett.* **97** 203106
[14] Zhang H, Tang D Y, Zhao L M, Bao Q L and Loh K P 2009 *Opt. Express* **17** 17630
[15] Liu H, Luo A P, Wang F Z, Tang R, Liu M, Luo Z C, Xu W C, Zhao C J and Zhang H 2014 *Opt. Lett.* **39** 4591
[16] Li L, Su Y L, WangY G, Wang X, Wang Y S, Li X H, Mao D and Si J H 2016 *IEEE J. Sel. Top. Quantum Electron.* **23** 1100306
[17] Liu W J, Pang L H, Han H N, Liu M L, Lei M, Fang S B, Teng H and Wei Z Y 2017 *Opt. Express* **25** 2950
[18] Shao H H, Liu Y M, Zhou X Y and Zhou G H 2014 *Chin. Phys. B* **23** 107304
[19] Li L, Yan P G, Wang Y G, Duan L N, Sun H, and Si J H 2015 *Chin. Phys. B* **24** 124204
[20] Li L, Wang Y G and Wang X 2017 *Laser Phys.* **27** 085104
[21] Luo Z C, Liu M, Guo Z N, Jiang X F, Luo A P, Zhao C J, Yu X F, Xu W C and Zhang H 2015 *Opt. Express* **23** 20030
[22] Xu Y H, Wang Z T, Guo Z N, Huang H, Xiao Q L, Zhang H and Yu X F 2016 *Adv. Opt. Mater.* **4** 1223
[23] Jiang X T, Liu S X, Liang W Y, Luo S J, He Z L, Ge Y Q, Wang H D, Cao R, Zhang F, Wen Q, Li J Q, Bao Q L, Fan D Y and Zhang H 2018 *Laser Photon. Rev.* **12** 1700229
[24] Lu L, Tang X, Cao R, Wu L M, Li Z J, Jing G H, Dong B Q, Lu S B, Li Y, Xiang Y J, Li J Q, Fan D Y and Zhang H 2017 *Adv. Opt. Mater.* **5** 1700301
[25] Lu B L, Chen H W, Guo J X, Jiang M, Zhang R J, Bai J T and Ren Z Y 2011 *Opt. Commun.* **284** 5353
[26] Novoselov K S, Geim A K, Morozov S V, Jiang D, Zhang Y, Dubonos S V, Grigorieva I V and Firsov A A 2004 *Science* **306** 666
[27] Liu N and Luo F 2008 *Adv. Funct. Mater.* **18** 1518
[28] Chen T, Liao C R, Wang D N and Wang Y P 2014 *Appl. Opt.* **53** 2828
[29] Sobon G, Sotor J, Jagiello J, Kozinski R, Zdrojek M, Holdynski M, Paletko P, Boguslawski J, Lipinska L and Abramski K M 2012 *Opt. Express* **20** 19463
[30] Sun Z P, Hasan T, Torrisi T, Popa D, Privitera G, Wang F Q, Bonaccorso F, Basko D M and Ferrari A 2010 *ACS Nano* **4** 803
[31] Liu X M, Cui Y D, Han D D, Yao X K and Sun Z P 2015 *Sci. Rep.* **5** 9101
[32] Kadir N A A, Ismail1 E I, Latiff A A, Ahmad H, Arof H and Harun S W 2017 *Chin. Phys. Lett.* **34** 014202
[33] Duan L N, Wang H S, Bai J, Wang Y G, Wei L L, Chen Z D, Yu J, Wen J and Li Y 2017 *Opt. Eng.* **56** 116104
[34] Li K X, Song Y R, Tian J R, Yang H and Yu G 2017 *Opt. Laser Technol.* **96** 18
[35] Xu J, Wu S, Liu J, Wang Q, Yang Q H andWang P 2012 *Opt. Commun.* **285** 4466
[36] Wu X, Tang D Y, Zhang H and Zhao L M 2009 *Opt. Express* **17** 5580
[37] Haiml M, Grange R and Keller U 2004 *Appl. Phys. B* **79** 331
[38] Zhang X M, Gu C, Chen G L, Sun B, Xu L X, Wang A T and Ming M 2012 *Opt. Lett.* **37** 1334
[39] Ismail M A, Harun S W, Zulkepely N R, Nor R M, Ahmad F and Ahmad H 2012 *Appl. Opt.* **51** 8621
[40] Liu Z B, He X Y and Wang D 2011 *Opt. Lett.* **36** 3024
[41] Xia H, Li H, Wang Z G, Chen Y F, Zhang X X, Tang X and Liu Y 2014 *Opt. Commun.* **330** 147
[42] Popa D, Sun Z, Hasan T, Torrisi F, Wang F and Ferrari A C 2011 *Appl. Phys. Lett.* **98** 073106
[43] Li H P, Xia H D, Wang Z G, Zhang X X, Chen Y F, Zhang S J, Tang X G and Liu Y 2014 *Chin. Phys. B* **23** 024209